Chapter Number

NIR Single photon detectors with up-conversion technology and its applications in quantum communication systems

Lijun Ma, Oliver Slattery, and Xiao Tang
Information Technology laboratory, National Institute of Standards and Technology
United States of America

1. Introduction

The performance of a quantum communication system depends on both the transmission loss and detection efficiency. For current fiber-optic bases systems, the transmission loss is small in near the infrared (NIR) range, and many fiber-based communication systems and devices have tended to use this wavelength range. Therefore, the 1310 nm and 1550 nm bands have become the mainstream telecom wavelength windows. However, the most efficient and low cost single photon detectors, such as silicon based avalanche photodiodes (APD), do not work at this NIR wavelength range.

In current systems, three mainstream types of single photon detectors are used: photocathode-based detectors, APD based detectors and superconducting-based detectors. In photocathode-based detectors, an InGaAs/InP based photomultiplier tube (PMT) or InGaAs based Microchannel plate (MCP) can be used for single photon detection in the NIR range. For APD-based detectors, only InGaAs/InP based APD can work in this range. Almost all superconducting-based detectors work in the NIR, and according to different work method, superconducting-based detectors have two types of detector: Transition Edge Sensor (TES) and Superconducting Single-Photon Detector (SSPD). In addition to these mainstream detectors, single photon detection at NIR can be achieved using a technique known as frequency up-conversion. We discuss this alternative technique in detail in this chapter.

PMT, first invented in the 1930's, is used in many scientific applications, especially in those that require very large photosensitive areas. The wavelength sensitivity of PMTs is determined by the coating of the photocathode. While many suitable materials are available for visible light and UV-sensitive photocathodes, NIR sensitivity is not easily attainable. Currently, only an InGaAs/InP based PMT, that was developed by Hamamatsu, can reach the NIR range, but its performance is limited by very low quantum efficiency (QE) (1 % at 1600 nm) and large timing jitter (1.5 ns) [Hamamatsu, 2005]. MCP is micro-capillary electron multiplier. The Capillaries are coated with electron-emissive material and multiply photo-excited electrons from photon cathode [Wiza, 1979]. MCP usually has faster rise times and lower timing jitter than is achievable in PMT. However, similar to PMT, its most

suitable working wavelength range is in the visible light range, and only InGaAs MCP can work in the NIR range and, like PMTs, are limited with low QE (~1 %) [Martin, J. & Hink P. 2003].

APD is a solid-state counterpart of PMT, which was initially studied in 1960s [Goetzberger et al, 1963]. In an APD, a photon is absorbed in a bulk semiconductor, where it generates an electron-hole pair. With a sufficiently high electric field , carriers would be accelerated to speeds where they can generate more electron-hole pairs though impact ionization, resulting in an avalanche multiplication. The Si-based APD (Si-APD) is the most practical and widely used single photon detector in the recent years. It has very high QE with low noise level in visible light range and can work at room temperature. However, its QE decreases rapidly at wavelengths approaching NIR (i.e. longer than 1000 nm) and it does not work at the two telecom bands (1310 nm and 1550 nm). InGaAs/InP based APDs do work in NIR but there are significant limitations. The ionization coefficient for electrons and holes in InGaAs are comparable, which would lead to a higher dark counts (a measure of the noise level in the detector) in the finite gain mode [Lacaita et al., 1996]. To reduce this noise, the APD should be operated at very low temperatures. However, the cut-off wavelength of InGaAs shortens as the temperature decreases: and the device loses sensitivity to 1550-nm photons at around -100 °C. Furthermore, trapped carriers in the device cause a severe afterpulse problem in this type of APD, especially at lower temperatures as the trapping lifetime becomes longer. Therefore, the operating temperature for this type of APD is set at somewhere between -100 °C and -20 °C where the total dark count rate (combining those due to thermal generation and those due to the afterpulse) is low and the detection range reaches to the desirous wavelengths. To overcome the severe influence of afterpulsing, commercial single photon counting modules based on InGaAs/InP APDs use active quenching and are operated in gated, or Geiger, mode. However, with the gated rate limited to about the MHz range, this cannot satisfy the requirement of high-speed quantum communications. Recently, a self-difference technique has been developed for InGaAs APDs that suppresses the afterpulsing noise, and it has been successfully applied to a GHz quantum communication system [Yuan et al., 2007]. The InGaAs APD has about 10 % detection efficiency, but it still has about 6 % afterpulse probability which would contribute extra errors to any quantum communications system.

For some time now, superconducting technology has been used to implement single photon detectors [Gol'tsman et al., 2001; Hadfield et al., 2007; Takesue et al., 2007; Lita et al., 2008; Ma et al., 2009]. These type of detectors can have extremely low dark count rates and flat wavelength sensitivity extending far into the infrared (IR) range. There are mainly two types of single photon detectors based on superconducting technology: TES and SSPD. TES, or TES microcalorimeter, consists of a piece of wolfram film, which is cooled below 100 mK. The film is kept at the transition edge of superconducting to normal conduction by Joule heating provided by the current from an associated circuit. In the TES detector, a photon is absorbed in the film producing a photoelectron which heats the electron system, raising its resistance and causing a drop in the current. The energy absorbed by the film is given by the integral of the drop in the current multiplied by the bias voltage. TES detectors have no intrinsic limitation of QE, and currently achieve almost 100 % QE at 1550. However, the timing jitter of a TES detector is quite large (~ 100 ns), and therefore it is not suitable for high

speed a quantum communications system. SSPD, or SNSPD (superconducting nanowire single-photon detectors), consists of a thin superconducting nanowire, which is meandered into a certain pattern. The detector is cooled into about 3 ^{o}K while the current in the nanowire is biased slightly lower than the critical current. When a photon is absorbed into the detection area, it will generate a hot spot. The current is forced to flow though a smaller cross-section of the nanowire around the hot spot, and therefore the current density exceeds the critical current density, which results in the loss of superconducting. After a few picoseconds, the hotspot disappears and the detector is restored to the original sate. SSPD has the advantages of very small timing jitter and a high counting rate in excess of a gigahertz. It also works in free-running mode, which is preferred for optimal performance of a quantum communication system. Because it must be operated at very low temperature, however, bulky and costly SSPD systems become a considerable impediment for practical applications.

A single photon detectors using frequency up-conversion technology, also called an up-conversion detector, is not a direct detection method. It uses a non-linear optical media to up-convert the frequency of photons in the NIR range to a shorter wavelength by a process known as sum frequency generation. The emerging photons, at visible wavelengths, are then detected using a visible region single photon detectors. Single photon detectors at the visible light region, such as the Si-APD, typically have high efficiency, low noise, can be operated in ambient temperatures, and are compact, inexpensive and practical. While, frequency up-conversion technology is not new [Midwinter & Warner 1967; Gurski, 1973], highly efficient conversion at single photon level has only recently been demonstrated by using periodically poled lithium niobate (PPLN) waveguides [Xu et al., 2007; Diamanti et al., 2005; Langrock et al., 2005; Thew et al., 2006; Tanzilli et al., 2005]. Up-conversion detectors work at room temperature, though the non-linear media is usually heated to a certain temperature to meet the phase matching condition. The internal conversion efficiency of the waveguide can reach as high as 100 %, and the total QE for this type of detector is about 20 % ~ 35 %. The frequency up-conversion process does not contribute any significant timing jitter. Instead, the timing jitter for this type of detector is influenced mainly by the Si-APD, and is usually in the region of 40 ps ~100 ps. Furthermore, the frequency up-conversion process provides some unique characteristics to the detector, such as narrow-band wavelength acceptance and polarization sensitivity, which are very useful for fiber-based quantum system. To date, several groups have successfully developed highly efficient up-conversion detectors for the NIR range and have employed them in high speed quantum communications systems.

Table 1 summarizes the performance and characteristics of the various single photon detectors in the NIR range, including their working temperature, maximum count rate, QE, dark count rate (DCR) and timing jitter.

Single photon detectors	Temperature, ^{o} K	Maximum Count rate, Hz	QE, %	DCR, Hz	Timing jitter
PMT (Hamamatsu)	193	10^{7}	1%	160k	1.5 ns
MCP (Burle)	210	$1x10^{6}$	1%	100k	1 ns
InGaAs APD (id Quantique)	Peltier cooled	4×10^{6} (gated)	10%	10 k	60 ps

InGaAs APD (Toshiba, UK)	243	4×10^{8}	10%	10 k	60 ps
SSPD (NIST)	<3	10^{9}	1%	10	60 ps
TES (NIST)	<0.1	10^{5}	95%	400	100 ns
Up-conversion detector (NIST)	Room*	5×10^{6}	31%	25 k	100 ps

Table 1. Performance of single photon detectors responsive in NIR range. The data are from [Hamamatsu, 2005; Martin, J. & Hink P. 2003, Ma et al., 2009; Takesue et al., 2007; Yuan et al., 2007; Xu et al., 2007; Lita et al. 2008].
* Although the up-conversion system itself is operated at room temperature, the non-linearilt crystal is heated locally to satisfy the phase matching condition required for optimal condition.

In this chapter, we offer a general overview of the theoretical principles and experimental results of single photon detectors using frequency up-conversion technology, and its applications in quantum information systems. We begin with a brief introduction of the non-linear optics and their phenomena, especially the SFG generation in a quasi-phase matching (QPM) grating that is the basis of up-conversion technology We then describe single-photon detectors with up-conversion and some key techniques used to implement the detectors with high efficiency, low noise, and low dark count rate. Finally, we introduce some existing quantum information systems, or quantum key distribution systems, using the up-conversion detectors.

2. Frequency Up-conversion

2.1 Sum Frequency generation

Frequency up-conversion technology is based on a second-order non-linear sum frequency generation (SFG) process, in which two input photons (a signal and a pump photon) at different frequencies annihilate and one photon at their sum frequency is simultaneously generated in a second-order non-linear media as shown in Fig. 1(a). According to non-linear optics theory, this process can happen only if the following two conditions are satisfied.

$$\omega_s + \omega_p = \omega_o \tag{1(a)}$$

$$\vec{k}_s + \vec{k}_p = \vec{k}_o \tag{1(b)}$$

where ω_s, ω_p and ω_o are the angular frequencies of the signal, pump and the output light, respectively. $\vec{k}_s$, $\vec{k}_p$ and $\vec{k}_o$ are the wave vectors of the signal, pump and the output light. Eq. 1(a) indicates the condition of energy conservation and Eq. 1(b) indicates the condition of momentum conservation. The frequency sum generation process is illustrated in Fig. 1.

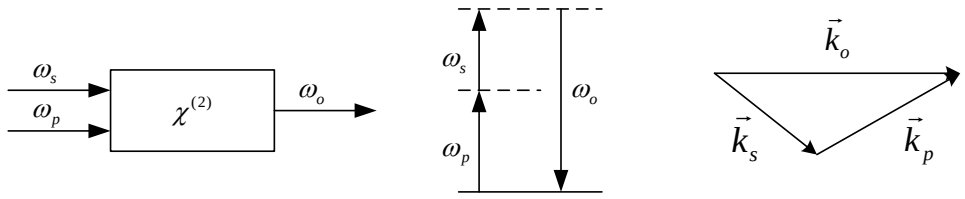

(a) (b) (c)

Fig. 1. Frequency up-conversion. (a) Geometry of the interaction. (b) Energy conservation condition. (c) Momentum conservation condition.

The nonlinear field evolution of the frequency sum generation process in a non-linear optical media can be described by

$$\frac{dE_s}{dz} = i\frac{\omega_s d_{eff}}{n_s c} E_o E_p^* \exp(i\Delta k \cdot z) \quad 2(a)$$

$$\frac{dE_p}{dz} = i\frac{\omega_p d_{eff}}{n_p c} E_o E_s^* \exp(i\Delta k \cdot z) \quad 2(b)$$

$$\frac{dE_o}{dz} = i\frac{\omega_o d_{eff}}{n_o c} E_s E_p \exp(i\Delta k \cdot z) \quad 2(c)$$

where E_s, E_p, and E_o are the electric field strengths of the signal, pump and output light, respectively; n_s, n_p and n_o are the indices of refraction at the three wavelengths; d_{eff} is the effective nonlinear coefficient of the crystal; c is the speed of light, and z is the longitudinal position along the propagation direction of the output light within the crystal. Δk represents the phase mismatch, which is defined by

$$\Delta k = \left| \vec{k}_o - \vec{k}_s - \vec{k}_p \right| \quad 3$$

At the perfect phase-matching condition, Δk equals to zero.

Single-photon up-conversion detectors use the principle of SFG to convert the single photon signal light to a wavelength that is efficiently detectable by single photon counters such as a Si-APD. In this situation, the signal light is at single photon level. The pump power is much stronger than the signal ($E_p >> E_s$) and the intensity of pump power does not deplete significantly in the up-conversion process, resulting in the approximation $\frac{dE_p}{dz} \approx 0$. Therefore, the Eq. 2(a-c) can be reduced into two coupled first-order differential equations.

There is no input at the sum wavelength ($E_{o(z=0)}$=0), which is the initial condition for the equation. By solving the equations with at this initial condition, the probability of up-conversion (or its transfer function response in general) is given as follows:

$$P_o(z) \approx \sin^2(\alpha\sqrt{I_p}z) \tag{4(a)}$$

where α is the conversion coefficient of the non-linear media and can be estimated by the following equation:

$$\alpha \approx (\frac{\omega_s \omega_o d_{eff}^2}{n_s n_o c^2})^{1/2} \tag{4(b)}$$

From Eq. 4 (a, b), one can see that the up-conversion efficiency is a sinusoidal oscillation with respect to pump power. There is an optimal pump power, at which the conversion efficiency reaches the maximum. In the perfect condition of phase-matching, the conversion efficiency can be as high as 100%.

According to Eq. 4 (a,b), to obtain high conversion efficiency, we need to increase the pump intensity while maintain or even reduce the optimal pump power since stronger pump power can lead to more noise. Furthermore, it can be seen in Eq. 4(a) that a longer interaction length z will increase the conversion efficiency. Choosing materials with high non-linear coefficients is another option for increasing the conversion efficiency.

2.3. Birefringent phase matching

Based on the Eq. 1(a, b), we can further obtain the phase matching conditions as follows:

$$\omega_s + \omega_p = \omega_o \tag{5(a)}$$

$$n_s\omega_s + n_p\omega_p = n_o\omega_o \tag{5(b)}$$

Because all non-linear crystals have dispersive, (i.e. the reflective index is changed with wavelength), it is impossible to satisfy the Eq. 3(a, b) simultaneously, if the three light have the same polarization. In practice, one can use birefringence to satisfy the phase matching condition. A ray of light is decomposed into two rays (the ordinary ray, or o-ray and the extraordinary ray, or e-ray) when it passes through a birefringent material depending on the polarization of the light. Many optical materials are birefringent, which means the reflective index depends on the polarization of the light. In that case, one can select lights with different polarization direction and the crystal orientations to satisfy the Eq. 5 (a,b) and implement phase matching. The main two types of birefringence phase matching are Type I (e.g. o+o→e) or Type II (o+e→e).

The advantage of birefringence phase matching is that it is a perfect phase matching, Δk is zero in this case. However, the birefringence phase matching has several limitations

1. The wavelength selection is limited by the material birefringent reflective index and angles. Not all wavelengths can find a suitable material and angle to implement phase matching.
2. The most severe main problem for birefringent phase-matching is walk-off issue: where the e-ray and the o-ray travel in different directions. This walk-off limits interaction length.
3. The nonlinear coefficients for the birefringent phase-matching conversion process are relatively low. For example, the largest coefficient for the birefringent phase-matching in lithium niobate crystal is only -4.64 pm/V (d_{31}).

Due to the above limitations, birefringent phase matching can not implement high efficient frequency conversion, and therefore is not suitable for up-conversion detectors.

2.2. Quasi-phase-matching

To overcome these limitations of the birefringent phase matching, the pump beam, signal beam and output beam should all be collinear and aligned to the same polarization orientation, and therefore can overcome the walk-off problem and also can take advantage of larger non-linear coefficient. Specifically, all the beams are in the extraordinarily polarization mode, and therefore the highest nonlinear coefficient, d_{33} = -40 pm/V, can be used, which is an order of magnitude higher than d_{31}. However, it is impossible to satisfy the perfect phase-matching condition shown in Eq. 5 (a, b), and therefore we need to use another scheme called quasi-phase-matching.

To explain the quasi-phase-matching technique, we go back to the Eq. 2 (a-c). If all light beams are collinear and have the same polarization orientation, there are no any birefringent phase-matching and $\Delta k_Q \neq 0$. In this case, the "sign" of dE_o/dz is flipped when z changes by $\pi / \Delta k_Q$, resulting in the periodic cancellation of the electrical filed strength of the output beam, E_o, and have no output of E_o. By reversing the domain poles every $\pi / \Delta k_Q$, the quasi-phase-matching technology contributes to the "sign" alternative over the same period, ensuring that there is positive energy flow from the signal and pump frequencies to the output frequencies even though all the frequencies involved are not phase locked with each other. The electrical field strength of output beam versus longitudinal position with and without periodical poling are shown in fig. 2. Since the typical period for complete conversion to the output filed in on the order of thousands of poling downs, the evolution of the output field is well characterized by a sine function of the longitudinal position. Therefore, we can ignore the small fluctuation illustrated in the fig. 2 and approximate the full up-conversion process for the poled system with Eq. 4 (a, b)

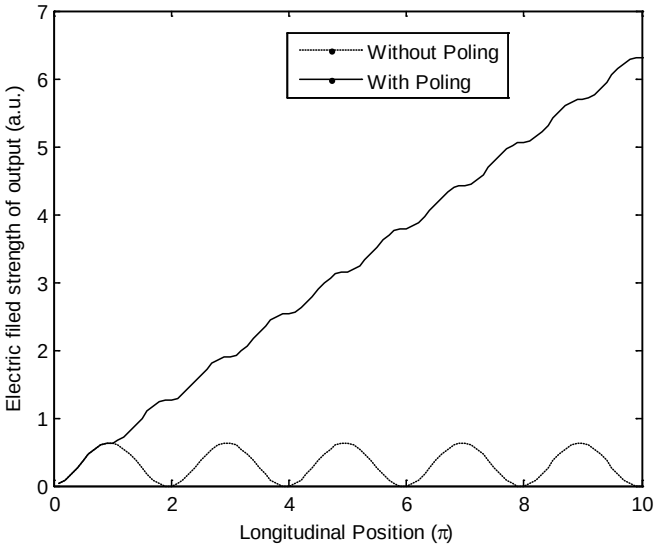

Fig. 2. Electric field strength of output light versus longitudinal position with poling and without poling.

From the phase view, the periodical "sign" change results in an extra term ($2m\pi/\Lambda$) in Eq. 3. Because all three beams are collinear, their wavevectors have the same direction, and values are their wave numbers. We are able to show the phase relation in one dimension in Fig 3.

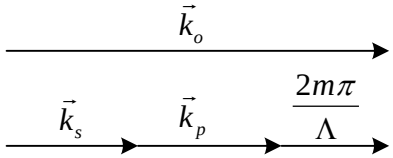

Fig. 3. Phase-match condition in quasi-phase-matching.

The phase mis-matching is determined by the Eq. 6.

$$\Delta k \equiv k_o - k_s - k_p - \frac{2m\pi}{\Lambda} \tag{6}$$

where k_s ,k_p ,k_o are the wave numbers of the signal, pump and output beams in the crystal; Λ is the poling period for the m^{th} order quasi-phase-matched condition of the nonlinear PPLN waveguide. By properly selecting Λ, the poling period of the crystal, the quasi-phase-matching is satisfied ($\Delta k = 0$). In the most desirable first-order (m=1) quasi-phase-matching condition, the ideal period can by calculated using the following equation:

$$\Lambda = 2\pi/(k_o - k_s - k_p) \quad (7)$$

Once the ideal period, Λ, is calculated, a suitable mask can be designed with the ideal period imprinted and a photo-lithographic technique may then be used to make a periodic pattern on a nonlinear material substrate. When the substrate is heated and an intense electric field applied to the region exposed by the mask, the electrical field flips the direction of the nonlinear susceptibility of the crystal. After annealing, the periodically poled material is ready to use. More accurate tuning of the Λ is achieved by adjusting the crystal temperature since the refraction index is a function of temperature.

In the quasi-phase-matching, the phase is not perfectly matched in each poling period but it ensures that positive energy transfers from the signal and pump frequencies and is converted to the output frequencies in the whole optical length of the crystal. Due to the imperfect phase matching in each poling period, the effective nonlinearity is reduced and can be estimated by the following equation:

$$d_{eff} = (\frac{2}{\pi})(\frac{1}{m})d_{33} \quad (8)$$

All even number orders (m=2, 4, 6…) of quasi-phase-matching will have no output since periodical cancellation of the electrical filed strength of output light will occur. For all odd number orders (m=1,3,5…), according to Eq. 8, the first-order (m=1) quasi-phase-matching has the highest effective nonlinear coefficient, though it is relatively hard to fabricate since the periods are shorter. Third-order (m=3) quasi-phase-matching, on the other hand, is often used as the longer periods are easier to fabricate. Because d_{33} is much larger than d_{31} in lithium niobate, the effective nonlinear coefficient in third order quasi-phase matching is larger than that in birefringent phase matching.

Quasi-phase-matching can remove constraint on finding wavelengths and angles that phase match, and allow use of the highest nonlinear coefficient. The most advantage of the quasi-phase-matching technique is the elimination of walk-off and the subsequently longer allowable interaction distance within the crystal. Furthermore, all three beams can be coupled together into a crystal waveguide, in which a higher beam intensity and longer interaction distance leads to significantly higher conversion efficiency.

The quasi-phase-matching in periodically poled lithium niobate allows us to take advantage of the larger d_{33} nonlinear coefficient. Furthermore, when the PPLN is implemented into a waveguide, a higher intensity of pump can be provided and a longer interaction distance becomes possible. Currently, PPLN waveguides are the most suitable devices to implement frequency up-conversion with almost 100% internal conversion efficiency achievable with relatively low noise.

3. NIR Up-conversion detector

Recently, several highly efficient up-conversion single photon detectors for the NIR range have been demonstrated using PPLN waveguides [Xu et al., 2007; Diamanti et al., 2005; Langrock et al., 2005; Thew et al., 2006; Tanzilli et al., 2005] and bulk PPLN crystals [Vandevender & Kwiat, 2004]. In this section, we will describe in detail an up-conversion detector developed at NIST [Xu et al., 2007] and analyze its characteristics.

3.1 Up-conversion detector configuration

The NIST detector is designed to detect single photons at 1310 nm using a pump at 1550 nm. The signal photons are then converted to 710 nm and then detected by a Si-APD

The configuration of the NIST up-conversion detector is shown in Fig. 4. A 1550-nm CW laser provides the pump seed. If needed, the seed light can be modulated to an optical pulse train by a synchronized signal. This feature is similar to an optical gate, which is very useful for noise reduction or high speed gating operation in a communication system. The modulated 1550 nm pump seed is then amplified by an erbium-doped fiber amplifier (EDFA) (IPG: EAR-0.5K-C). Two 1310/1550 wavelength division multiplexer (WDM) couplers with a 25 dB extinction ratio are used to clean up the 1550 nm pulsed pump, specifically suppressing any EDFA noise that may extend to 1310 nm. The amplified 1550 nm pump light is then combined with a weak 1310 nm signal by another WDM coupler and the combined pump and signal are then coupled into the PPLN waveguides. The input polarization state of both the signal and the pump are adjusted by the polarization controllers, PC1 and PC2 respectively, to align with the polarization of waveguide before entering the coupler. From the Eq. 2, we know that a longer waveguide will require less pump power to reach the maximum conversion efficiency. The PPLN waveguide in the NIST up-conversion detector is 5 cm,the longest possible with current manufacturing capability. The input of the PPLN waveguide is fiber coupled, while the output is to free-space with a 710nm anti-reflection (AR) coating on the output end of the waveguide to increase transmission of the converted output signal. In addition to the 710 nm (SFG) up-converted weak light signal, the output of the PPLN waveguide consists of residual 1550 nm pump light and its second harmonic generation (SHG) 775 nm light. These beams are separated by two dispersive prisms and the 710 nm photons are detected efficiently by a Si-APD (PerkinElmer: SPCM-AQR-14). An iris and a 20 nm band-pass filter (Omega Optical, Inc.: 3RD700-720) are used to reduce any additional noise, such as that from photons leaked from into the system from the environment.

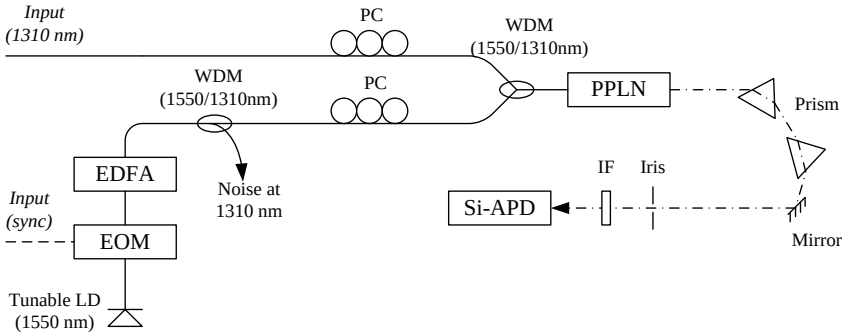

Fig. 4. Schematic diagram of the up-conversion detector. EOM: Electric-optic modulator; EDFA: Erbium-doped fiber amplifier; WDM: Wavelength-division multiplexing coupler; PC: Polarization controller; PPLN: Periodically-poled LiNbO3 waveguides; IF: Interference filter. Solid line: Optical fiber; Dash line: Free space optical transmission.

3.2 Detection efficiency

Detection efficiency is the one of the most important criteria in single photon detectors. The overall detection efficiency of an up-conversion detector is determined by the internal conversion efficiency in the PPLN waveguide, the coupling loss and component insertion loss , as well as the detection efficiency of Si-APD at the converted wavelength. The overall detection efficiency of an up-conversion detector can be estimated by the following formula:

$$\eta_o = \eta_{loss} \cdot \eta_{con} \cdot \eta_{\det} \approx \eta_{loss} \cdot \eta_{\det} \cdot \sin^2(\alpha \cdot \sqrt{P_{pmup}} \cdot L) \qquad 9$$

where η_o is the overall detection efficiency of the up-conversion detector; η_{loss} is the total loss in the detector, including the component insertion loss and waveguide coupling loss; η_{con} is the internal conversion efficiency in the PPLN, and can be estimated by Eq. 4; and $\eta_{\det}$ is the detection efficiency of Si-APD at the converted wavelength, which is 710 nm in our case. According to the specification of the Si-APD used in the NIST up-conversion detector, $\eta_{\det}$ is about 65%.

In a complete up-conversion detector unit, the insertion and coupling loss, the detection efficiency of the Si-APD and the structure of the waveguide are fixed. Therefore, the overall conversion efficiency of the detector is determined by the internal conversion efficiency of the waveguide, which is dependent on the pump intensity with a $\sin^2(\sqrt{\ })$ relationship according to Eq. 9. The measured conversion efficiency versus pump power in a CW mode

and in a pulsed pump mode is shown in Fig. 5. The measured results are in good agreement with the estimated value from Eq. 9. The maximal detection efficiency is 32 % for both pump modes, which corresponds to 100 % internal conversion efficiency after we exclude the insertion loss and the detection efficiency of Si-APD.

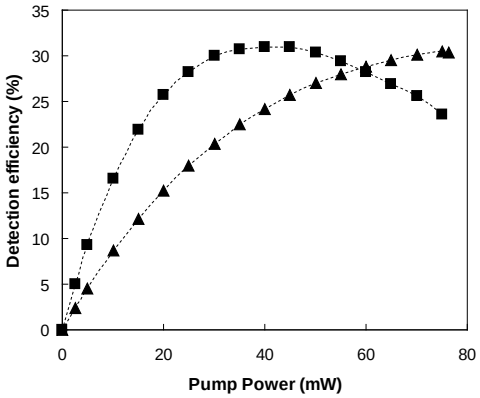

Fig. 5. The detection efficiency as a function of pump power. Two cases are studied: CW pump (triangle) and pulsed pump (square).

In many quantum information systems, the photons arrive with a synchronized classical signal. Therefore, the up-conversion detector can be operated in pulsed pump mode using the synchronized signal. The detection efficiency measured here is from a 625MHz synchronized classical signal with 600 ps (FWHM) pulses. The quantum optical pulse is pumped with the same synchronized signal but has a shorter 300 ps (FWHM) pulse width. The detector operating in pulse pump mode can reach the maximum conversion efficiency with a lower average pump power, which helps to reduce the noise (we discuss this in some detail in the next section). In these cases where there is not a synchronized signal, a CW pump is needed. For pulse and CW pump modes, the optimal pump power (average) is about 38 mW and 78 mW, respectively.

3.3 Noise reduction

For a single photon detector, the noise level, or dark count rate, is the most important performance parameter: a higher dark count rate can cause more errors in the quantum information system and degrade the system's fidelity.

The dark count rate has been extensively studied in frequency up-conversion technology [Xu et al., 2007; Diamanti et al., 2005; Langrock et al., 2005; Thew et al., 2006], and these are three main causes: intrinsic dark counts of Si-APD, linearly induced noise photons that leak through the filter from the pump, and nonlinearly induced noise photons due to scattering by the strong pump. The intrinsic dark count rate of the Si-APD is listed in the manufacturer's product specification. It is about 100 c/s in our case. The linearly induced dark counts are caused by the photons in the spectral tail from the pump source, which

extends to the signal wavelength range. We use two WDM couplers to greatly suppress this noise. The nonlinear process that causes the dark counts is widely believed to be from the Raman scattering process, in which photons in the signal band are generated by the strong pump and then up-converted to the detection wavelength, though this has not been strictly proven. In this up-conversion detector unit, we use a 1550 nm laser as a pump, whose wavelength is longer than that of the quantum signal we want to measure. Because the anti-Stokes component of the Raman process is much weaker than the Stokes component, a dark count rate of less than 2400 c/s is achieved when the conversion efficiency is maximized.

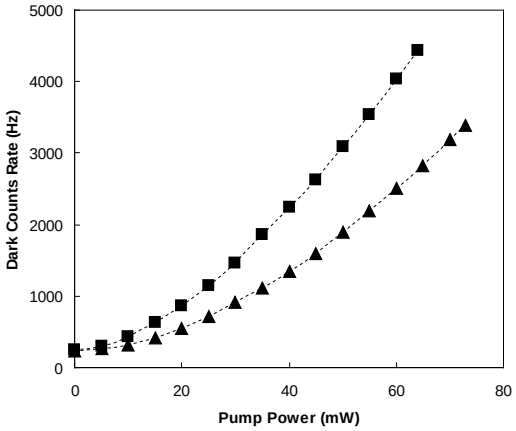

Fig. 6. The dark count rate as a function of pump power at the PPLN input. Two cases are studied: CW pump (triangle) and pulsed pump (square).

As shown in the Fig. 6, the pulse pump generates more dark counts than the CW pump for a given average power since the peak power of the pulse pump is higher than the average power. We refer to pump power as the average power of the pump, because the pulse pump needs less power than the CW pump to achieve a given detection efficiency. Therefore, the pulse pump can achieve a given detection efficiency with less dark counts in comparison with CW pump. For example, the maximum detection efficiency is reached when using the pulse pump at 38 mW and the dark count rate is 2400 c/s. For the CW pump, a power of 78 mW is needed to achieve the maximum detection efficiency, which incurs a dark count rate of 3100 c/s. Consequently, a pulse pump can use lower power and effectively reduce the dark count rate compared to a CW pump

3.4. Wavelength and temperature response

When the quasi-phase matching condition in a PPLN waveguide is satisfied at a particular signal wavelength, the maximum up-conversion efficiency is achieved. When the signal is shifted from that wavelength the up-conversion efficiency is reduced. This means that the

up-conversion detectors have a narrow wavelength acceptance width, and is similar to a narrow band pass filter. It helps to filter out noises at wavelengths other than the signal wavelength. However, this may be a drawback when the detector is used to measure signals with wider spectrum. The acceptance spectral width of the up-conversion detector is determined by the transfer function response of the PPLN waveguide. The transfer function response of a finite-length uniform QPM grating in the waveguide is a function of a $\mathrm{sinc}^2(\ )$ as follows: [Fejer et al, 1992; Micheli 1997]

$$I_o(\Delta k_Q) \propto I_p \cdot I_s \cdot \mathrm{sinc}^2(A \cdot \Delta k_Q \cdot L) \qquad 10$$

where I_o, I_p, I_s are the intensity of SFG, pump, and signal beam; A is a constant; L is the waveguide length; and Δk_Q is the phase-mismatching, which can be calculated by the following relation with the system wavelengths as follows.

$$\Delta k_Q = \frac{n_o}{\lambda_o} - \frac{n_p}{\lambda_p} - \frac{n_s}{\lambda_s} - \frac{m}{\Lambda} \qquad 11$$

where λ_o, λ_p and λ_s are the wavelengths for output, pump, and signal, respectively, and n_o n_p and n_s are the reflective index for the three wavelength. Λ is the poling period for the mth order quasi phase matched condition of the nonlinear PPLN waveguide. According to Eq. 2 and 3, the acceptance spectral width is dependent on the length of he waveguide. The longer the waveguide is, the narrower the acceptance spectral width will be. Fig. 7 shows the measured detection efficiency as a function of signal wavelength at certain fixed pump wavelength and temperature. From the figure, we can see that the spectrum is similar to the $\mathrm{sinc}^2(\ )$ function and the acceptance spectral width of the main peak is about 0.25 nm (FWHM). If we use a short waveguide or a pump light with wider spectrum, the acceptance spectral width can be broadened.

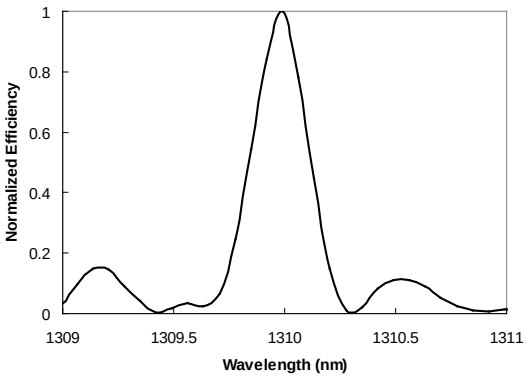

Fig. 7. The normalized detection efficiency as a function of signal wavelength, when the pump wavelength and temperature of the waveguide are fixed.

The up-conversion wavelength peak is also temperature sensitive. Therefore, one or both of the pump and the signal wavelength, as well as the waveguide temperature needs to be accurately tuned to achieve the maximum up-conversion efficiency. To investigate the temperature sensitivity of the up-conversion, we sent a 1-mW CW 1310 nm laser beam with a linewidth less than 10 MHz into the PPLN waveguide. Moreover, we turned off the pump seed laser so that the amplified spontaneous emission (ASE) noise from the EDFA acted as the pump. Using an optical spectrum analyzer (OSA), we measured the spectrum at the output of PPLN waveguide at different temperatures from 50°C to 70°C. The output spectrum is normalized to the peak power after we subtracted the ASE spectrum. The result is shown in Fig.8.

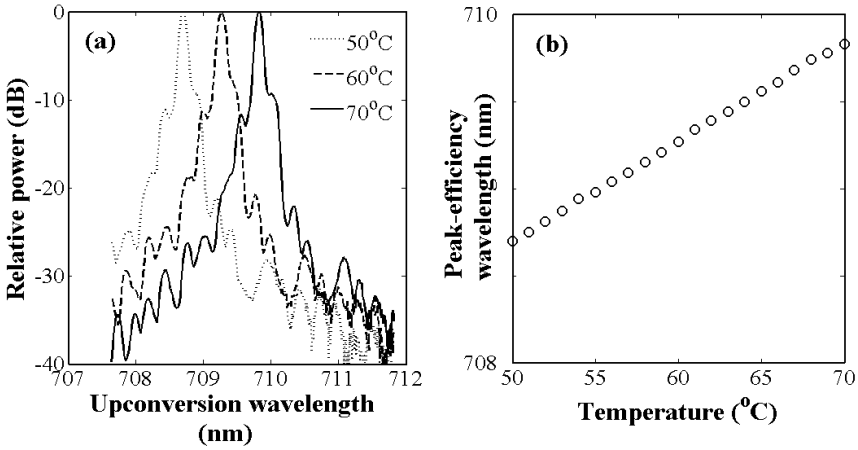

Fig. 8 (a) The normalized output spectrum of the PPLN at the different temperatures shown in inset. (b) The up-conversion wavelength peak as a function of temperature.

As shown in Fig. 8(a), the spectral width of the sum frequency at 710 nm is about 0.15 nm. The result is consistent with the spectral width of 0.25 nm for the signal at 1310 nm as shown in Fig. 7. Also from Fig 8(a), the peak wavelength is shifted as the temperature changes, which means that the quasi-phase matching condition can be achieved by either varying the converted wavelength (via tuning of the pump wavelength and/or signal wavelength), or varying the waveguide temperature, as shown in Fig. 8(b). Within a temperature variation range of 20 degrees, the central wavelength for maximal efficiency linearly varies by approximately 1.1 nm. The temperature response of the waveguide provides a method to tune the up-conversion detector to reach to the maximum detection efficiency, even if the signal and pump wavelengths are fixed.

3.5 Polarization characteristic

The up-conversion process in a PPLN waveguide is polarization sensitive. If its polarization extinction ratio is sufficiently high, the device can be used as a polarizer. This feature is very useful in polarization-encoding quantum communications systems. Fig. 9 shows the dependence of detection efficiency on the polarization direction of an input signal at 1310 nm. The deviation angle is the angle (in Jones space) between the given input polarization state and the one at which the conversion efficiency is maximum. We also compared the measurement results with a $\cos^2(\ )$ curve, the function which represents an ideal polarizer. The curve agrees well with the measured data and we believe that the slight difference is caused by the measurement uncertainty of the polarimeter. As shown in the Fig. 6, the polarization extinction ratio of the PPLN is over 25 dB. Therefore, an up-conversion detector can be used as a polarizer in a polarization-based quantum information system, and therefore avoids the additional insertion loss that an otherwise required polarizer would add.

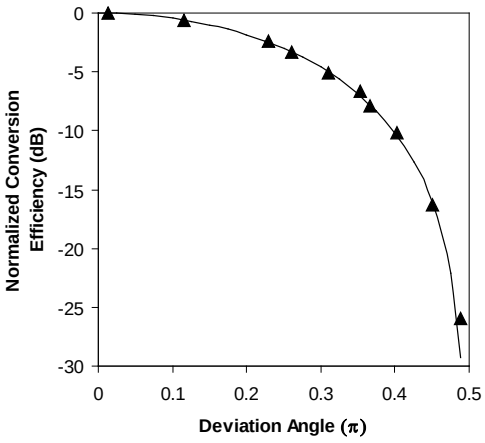

Fig. 9. The normalized conversion efficiency of the PPLN waveguide as a function of deviation angle of the input signal at 1310 nm. The deviation angle is the angle between the given polarization state and the state at which the conversion efficiency is maximized. Triangle: Measurement results; Solid line: $\cos^2()$ curve

4. Application in quantum communication systems

Quantum communication, or quantum key distribution (QKD), is a technique for developing secure encryption keys over unsecured communication channels that is guaranteed by the fundamental quantum properties of single photons instead of mathematical complexity for the basis of security [Gisin et al., 2002]. It is not possible to make a perfect copy (clone) of an unknown quantum state, thus precise measurement by an eavesdropper is not achievable. The Heisenberg uncertainty principle states that pairs of quantum properties cannot be precisely measured simultaneously; for example, position and momentum. Horizontal-vertical and diagonal polarization of photons is another such pair.

QKD systems use quantum states, such as polarization, to encode information on single photons. An initial random key is established by randomly encoding state information on these photons, sending the photons to and recovering the encoded state information at the other end of the link. After sifting, error correction and privacy amplification, the three signal processing procedures, the initial (raw) keys become secure keys and ready for use.

The idea to use quantum states to securely encode information originated with Stephen Wiesner in 1983 [Wiesner, 1983]. This idea was taken forward by Charles Bennett and Gilles Brassard in 1984 [Bennett & Brassard, 1984] to develop the famas QKD protocol called BB84, which uses four quantum states. In 1992, Charles Bennett proposed a simplified version of the protocol, named B92, [Bennett, 1992] that uses only two quantum states. These two protocols are commonly used in most QKD systems today. The first demonstration of a QKD system was completed in 1989, in which the quantum channel was a 30-cm long path of air in the laboratory [Bennett & Brassard, (1989)]. Since then, a number of groups have successfully developed many experimental QKD systems, which were described in a comprehensive review article [Gisin et al., 2002].

Single photon detector is one of the key elements for a QKD system since it encodes information on quantum state of single photons. Among all available types of single photon detector, up-conversion detector is a quite suitable device for QKD systems, due to its high detection efficiency, low dark count rate and unique characteristics, such as narrow acceptance spectral width and polarization sensitivity. Its advantages are listed as following:

1. High detection efficiency: many QKD systems use narrow linewidth attenuated laser light as the single photon source, which is much narrower than the acceptance bandwidth of up-conversion detection. Therefore, an up-conversion detector can reach its max detection efficiency, and results in a higher secure key rate.

2. Low dark count rate: many QKD system recover clock from their classical channel, which can be used as the synchronized trigger signal for the pulse pump operation in the up-conversion detector, which can lead to a lower dark count rate and, therefore, a lower error rate in the system.
3. Narrow acceptance spectral width: each up-conversion detector has a relatively narrow acceptance spectral width that functions as a band-pass filter, rejecting the noise due to crosstalk from strong signals in classical channel that may shares the same fiber.
4. Polarization sensitivity: this feature can be used as a polarizer, which avoids the additional insertion loss that an extra polarizer would add.

Because of these outstanding performance characteristics, several research groups have successfully demonstrated fiber-based QKD systems using up-conversion single photon detectors. By way of an example, we introduce a fiber-based QKD system developed at NIST. The system uses the B92 protocol [Xu et al. 2007] with 1310 nm photons that share a single optical fiber with bi-directional classical signals at the 1550 nm band.

A QKD system using the B92 protocol requires two detectors to detect the photons emerging from the two different measurement bases. Fig. 10 outlines a compact dual up-conversion detector system, and is an all fiber system rather than the free-space output configuration described in Fig. 3. A weak pump seed laser is amplified by an EDFA and split into two parts, each of which will provide the pump for one of the detectors. Each detector in this dual detector system consists of a 5 cm PPLN waveguide, whose input and output are fiber coupled. The detectors use in-line narrow band-pass filters to suppress noise from the pump light and its SHG component. The dual up-conversion detector is packaged into a rack-mounted box and integrated into the QKD system. This all fiber detector is easy to use and more compact compared to the free space output detector described earlier, however its overall detection efficiency is reduced to 15~20%, due to output coupling loss from the waveguide to the fiber and the insertion loss associated with the narrow band-pass filters.

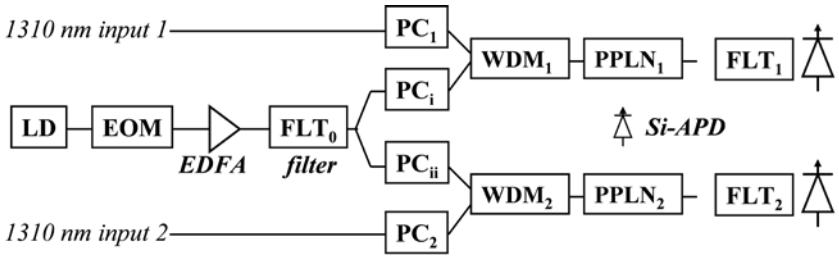

Fig. 10. The configuration of compact dual up-conversion detectors. LD: Laser diode; EOM: Electric-optic modulator; EDFA: Erbium-doped fiber amplifier; FLT: Optical filter; PC: Polarization controller; WDM: Wavelength-division multiplexer for 1310 nm and 1550 nm; PPLN: PPLN waveguide.

The configuration of the QKD system using the up-conversion detector is shown in the Fig. 11. The QKD system uses a custom printed circuit board with a field-programmable gate array (FPGA) [Mink et al., 2006] to generate a random stream of quantum key data and to transmit and receive the classical data. The classical data is carried by an optical signal at 1550 nm.

To polarization-encode the quantum channel with the random data, we first modulate a 1310-nm CW light into a 625 MHz pulse train which is evenly split into two polarization channels. Each pulse train is further modulated by one of two complementary 625 Mbit/s quantum channel data streams. The two quantum channels are combined by a 45-degree polarization-maintaining combiner and attenuated to a mean photon number of 0.1 per bit, and then multiplexed with the classical channel before being coupled into a standard single-mode fiber for communication.

At Bob, another WDM is used to demultiplex the quantum and the classical channels. The quantum channel is polarization-decoded and detected using the up-conversion single-photon detectors, generating the raw key. Bob's board informs Alice of the location of the raw keys via the classical channel. After reconciliation and error correction [Nakassis et al., 2004], Alice and Bob obtain a common version of the secure keys, which are further used to encode and decode the classical signal.

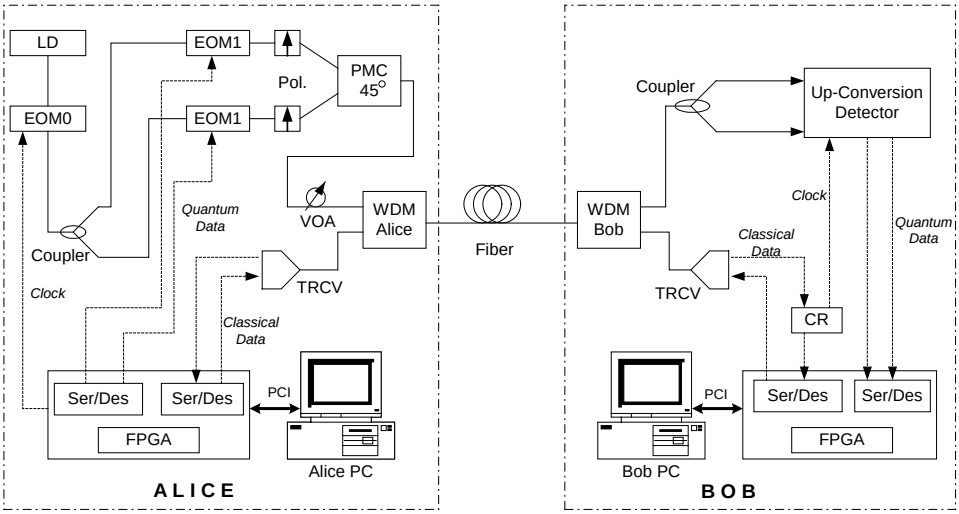

Fig. 11. The B92 polarization coding QKD system. LD: Laser diode; EOM: Electric-optic modulator (LiNbO3); PC: Polarization controller; PMC-45°: Polarization maintaining combiner that combines two light signals that are separated by 45 degrees; VOA: Variable optical attenuator; WDM: Wavelength-division multiplexer; SMF: Standard single-mode fiber; TRCV: Optical transceiver; CR: Clock recovery module; FPGA: Custom printed circuit board controlled by a field-programmable gate array; PCI: PCI connection; Up-conversion detector: See Fig. 8; Dotted line: Electric cable; Solid line: Optical fiber.

One of the main concerns for any QKD system is the noise level, or dark count rate. Altough the up-conversion detector has a low dark-count rate, other sources of noise much be identified when the detector is integrated into a system. In the QKD system, the quantum channel (1310 nm) and the bi-directional classical channel (1510 nm & 1590 nm) share a single standard telecom fiber using WDM, so there is a concern that the quantum channel may suffer from noise from the classical channel. In a QKD system that uses up-conversion detectors the crosstalk from strong signal in classical channel (1510 nm & 1590 nm) will be strongly blocked by of the narrow acceptance spectral width of the up-conversion detector. In the classical channel, there are another two noise sources: the first is from the transceivers which emit a small amount of optical noise around 1310 nm and the second due to nonlinear effects, which is widely believed to be the Raman scattering although that has not strictly been proven. The strong signals at 1510 nm and 1590 nm interact with the fiber and, in an nonlinear anti-Stokes process, generate photons around 1310 nm.. These 1310 nm fiber generated photons enter the PPLN waveguides and are up-converted to 710 nm. Fig. 12(a) shows the extra dark count rate induced by the classical channel at various fiber link distances. We first measure the dark count rate when one or both of the classical transceivers are on, and then subtract the dark count rate measured when both transceivers are off. The photon leakage can be evaluated by the extra dark counts in a back-to-back (0 km) connection while the nonlinearly induced dark photon effect will vary over the transmission distance.

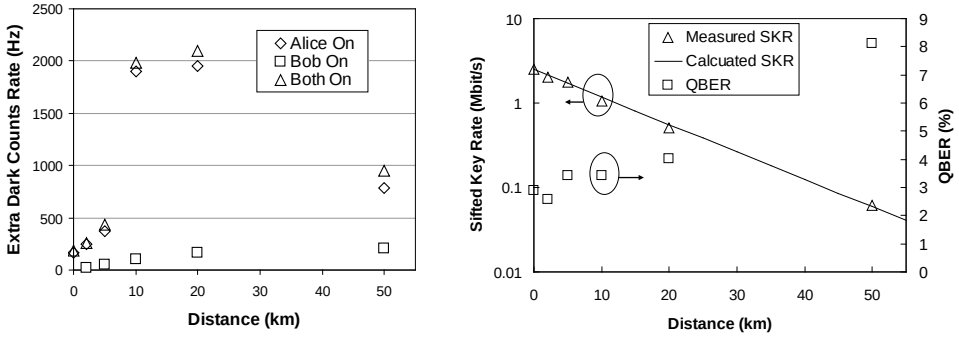

(a) (b)

Fig. 12. The extra dark count rate induced by the classical channel in the PPLN1 detector in three cases: Square, only the transceiver at Alice is on; Diamond, only the transceiver at Bob is on; Circle, both transceivers are on. The PPLN2 detector exhibits similar behaviors. (b) The system performance of the B92 polarization-based QKD system with the 1550 nm pumped up-conversion detector.

As shown in the Fig. 12(a), the photon leakage noise is small and the dark counts are mainly induced by the Raman anti-Stokes process, particularly from the classical signals at 1510 nm

propagating from Alice to Bob (forward anti-Stokes). The backward anti-Stokes noise is generated by the classical signals at 1590 nm propagating from Bob to Alice and is much weaker than the forward anti-Stokes because the 1590 nm light is further away from 1310 nm signal photons. During the first 20 km, the accumulated anti-Stokes effect is larger than the accumulated fiber loss. Therefore the dark count rate, primarily induced by the forward anti-Stokes effect, increases over to the first 20 km. After 20 km, the dark count rate reduces as the accumulated fiber loss becomes the dominant effect. The 1510 nm light is sufficiently attenuated by losses in the fiber so that the anti-Stokes noise is significantly reduced after 20 km. By comparison, dark counts induced by the backwards anti-Stokes effect also increases with transmission distance but, in the NIST system, it saturates after 20 km. This is because both the 1590 nm classical signal and backwards anti-Stokes effect are sufficiently attenuated by the fiber loss as the fiber length increases beyond 20 km. In general, the classical channel induces negligible dark counts into the QKD system, particularly from 1510 nm. A longer wavelength transceiver would greatly help to reduce the dark count rate further, but care must be taken to keep it within the standard telecom band.

The system performance is shown in Fig. 12(b). During our measurements, the pump power was fixed at 40 mW. The sifted-key rate is 2.5 Mbit/s for a back-to-back connection, 1 Mbit/s at 10 km, and 60 kbit/s at 50 km. The quantum bit error rate (QBER) is approximately 3% for the back-to-back configuration, remains below 4% up to 20 km, and reaches 8% at 50 km. The finite extinction ratio of the modulator and timing jitter of the system induces a background QBER of approximately 2.5% and the remaining QBER emanating from dark counts generated by both the pump light and the classical channel, as we described earlier. We also calculated the theoretical sifted-key rate and QBER and they agree well with the measured results. Although we fixed the pump power close to the maximum up-conversion efficiency, the QBER remains small until 20 km due to the low dark count rate of the 1550 nm up-conversion detector. The QKD system can generate secure keys in real time for one-time-pad encryption of continuous 200 Kbit/s encrypted video transmission over 10 km.

5. Conclusion

Frequency up-conversion single photon detectors use the principle of sum frequency generation to up-convert single photons in the near IR range to a shorter wavelength for an efficient detection with suitable detectors such as Si-APDs. The up-conversion detectors are usually operated at room temperature with high detection efficiency and a low dark count rate. The detectors have a very narrow acceptance spectral width and polarization sensitivity, properties that can be exploited in certain applications requiring narrow linewidth or polarization specific detection. These unique characteristics can be used to enhance system performance in some applications, including fiber-based quantum communications systems.

6. References

Bennett, C. H. & Brassard, G. (1984). Quantum cryptography: Public key distribution and coin tossing. *Proc. IEEE Int. Conf. Comput. Syst. Signal Process.*, pp. 175–179.

Bennett, C. H. & Brassard, G. (1989). The Dawn of a New Era in Quantum Cryptography: the Experimental Prototype is Working .*SIGACT NEWS,* Vol.20, pp. 78-83

Bennett, C. H. (1992). Quantum cryptography using any two nonorthogonal states. *Phys. Rev. Lett.*, Vol. 68, pp 3121-3124

Boyd, R. W. (2008). Nonlinear Optics, Academic Press, ISBN 978-0123694706, New York.

Diamanti, E.; Takesue, H.; Honjo, T.; Inoue, K. & Yamamoto, Y. (2005). Performance of various quantum-key-distribution systems using 1.55-μm up-conversion single-photon detectors. *Phys. Rev. A,* Vol. 72, 052311

Fejer, M.; Magel, G.; Jundt, D. & Byer, R. (1992). Quasi-phase-matched second harmonic generation: tuning and tolerances. IEEE J. Quantum Electron. Vol.28, pp 2631-2654

Gisin, N.; Ribordy, G.; Tittel, W. & Zbinden, H., (2002). Quantum cryptography. *Rev. Mod. Phys.* Vol. 74, pp 145–195

Goetzberger, A.; McDonald, B.; Haitz, R.H. & Scarlett, R.M. (1963). Avalanche effects in silicon p-n junctions. II. Strucrually perfect junctions. *J. Appl. Phys.* Vol 34: 1591-1600

Gol'tsman, G. N.; Okunev, O.; Chulkova G.; Lipatov, A.; Semenov, A.; Smirnov, K.; Voronov, B. & Dzardanov, A. (2001). Picosecond superconducting single-photon optical detector. *Appl. Phys. Lett.* Vol. 79, pp 705-707

Gurski, T. (1973). High-quantum-efficiency infrared up-conversion. *Appl. Phys. Lett.*, Vol. 23, pp 273-275.

Hadfield, R.; Schlafer, J.; Ma, L.; Mink, A.; Tang, X. & Nam, S. (2007). Quantum key distribution with high-speed superconducting single-photon detectors. *CLEO/QELS Technical Digest,* QML4,

Hamamatsu. (2005). Near infrared photomultiplier tube R5509-73 data sheet.

Korneev, A.; Kouminov, P.; Matvienko, V.; Chulkova, G.; Smirnov, K.; Voronov, B.; Gol'tsman, G. N.; Currie, M.; Lo, W.; Wilsher, K.; Zhang, J.; Słysz, W.; Pearlman, A.; Verevkin, A. & Sobolewski, R. (2004). Sensitivity and gigahertz counting performance of NbN superconducting single-photon detectors. *Appl. Phys. Lett.* Vol. 84, pp 5338-5340

Langrock, C.; Diamanti, E.; Roussev, R. V.; Yamamoto, Y.; Fejer, M. M. & Takesue, H. (2005). Highly efficient single-photon detection at communication wavelengths by use of upconversion in reverse-proton-exchanged periodically poled LiNbO3 waveguides. *Opt. Lett. Vol.* 30, pp. 1725-1727

Lacaita, A.; Zappa, F.; Cova, S. & Lovati, P. (1996) Single-photon detection beyond 1 μm: performance of commercially available InGaAs/InP detectors. *Appl. Opt.,* Vol. 35, pp 2986-2996

Lita, A. E.; Miller, A. J. & Nam, S. W. (2008). Counting near-infrared single-photons with 95% efficiency," *Opt. Express,* Vol. 16, pp3032-3040

Ma, L.; Nam, S.; Xu, H.; Baek, B.; Chang, T.; Slattery, O.; Mink, A. & Tang, X. (2009). 1310 nm differential phase shift QKD system using superconducting single photon detectors. *New Journal of Physics,* Vol. 11, pp 054020

Martin, J. & Hink P. (2003) Single-Photon Detection with MicroChannel Plate Based Photo Multiplier Tubes. *Workshop on Single-Photon: Detectors, Applications and Measurement Methods, NIST*.

Micheli, M. P. (1997) χ^2 effects in waveguides. *Quantum Semiclassic. Opt*, Vol. 9, pp 155–164.

Midwinter, J. & Warner, J. (1967) Up-conversion of near infrared to visible radiation in lithium-meta-niobate. J. Appl. Phys. Vol 38, pp 519-523

Mink, A.; Tang, X.; Ma, L.; Nakassis, T.; Hershman, B.; Bienfang, J. C.; Su, D.; Boisvert, R.; Clark, C. W. & Williams, C. J. (2006). High speed quantum key distribution system supports one-time pad encryption of real-time video. *Proc. of SPIE,* Vol. 6244, 62440M,

Nakassis, A., Bienfang, J. & Williams, C. (2004). Expeditious reconciliation for practical quantum key distribution. *Proc. of SPIE,* Vol. 5436, pp. 28-35.

Takesue, H.; Nam, S.; Zhang, Q.; Hadfield, R. H.; Honjo, T.; Tamaki, K. & Yamamoto, Y. (2007). Quantum key distribution over a 40-dB channel loss using superconducting single-photon detectors. *Nature Photonics*, Vol. 1, pp 343-348

Tang, X.; Ma, L.; Mink, A.; Nakassis, A.; Xu, H.; Hershman, B.; Bienfang, J.; Su, D.; Boisvert, R.; Clark, C. & C. Williams. (2006). Experimental study of high speed polarization-coding quantum key distribution with sifted-key rates over Mbit/s. *Optics Express*, Vol. 14, No.6, pp 2062-2070

Tanzilli, S.; Tittel, W.; Halder, M.; Alibart, O.; Baldi, P.; Gisin, N. & Zbinden, H. (2005). A photonic quantum information interface. *Nature,* Vol 437, pp 116-120

Thew, R. T.; Tanzilli, S.;, Krainer, L.; Zeller, S. C.; Rochas, A.; Rech, I.; Cova, S.; Zbinden, H. & Gisin, N. (2006). Low jitter up-conversion detectors for telecom wavelength GHz QKD. *New J. Phys.* Vol. 8, pp 32.

Vandevender, A. P. & Kwiat, P. G. (2004). High efficiency single photon detection via frequency up-conversion. *J. Mod. Opt.,* Vol. 51, 1433-1445

Wiesner, S. (1983). Conjugate coding. *Sigact News,* Vol. 15, pp 78-88

Wiza, J. (1979). Microchannel plate detectors. *Nuclear Instruments and Methods* Vol. 162: pp 587-601

Xu, H.; Ma, L.; Mink, A.; Hershman, B. & Tang, X. (2007). 1310-nm quantum key distribution system with up-conversion pump wavelength at 1550 nm. *Optics Express*, Vol 15, No.12, pp 7247- 7260

Xu, H.; Ma, L. & Tang, X. (2007). Low noise PPLN-based single photon detector. *Proceedings of SPIE.* Vol 6780, pp. 67800U-1

Yuan, Z. L.; Dixon, A. R.; Dynes, J. F.; Sharpe, A. W. & Shields, A. J. (2008). Gigahertz quantum key distribution with InGaAs avalanche photodiodes. *Appl. Phys. Lett.* Vol. 92, 201104.